

Contents lists available at ScienceDirect

Applied Mathematics and Computation

journal homepage: www.elsevier.com/locate/amc



Application of the dynamic Monte Carlo method to pedestrian evacuation dynamics



Nutthavuth Tamang, Yi Sun*

Department of Mathematics, University of South Carolina, Columbia, SC 29208, USA

ARTICLE INFO

Article history: Received 28 July 2022 Revised 9 December 2022 Accepted 17 January 2023

Keywords:
Pedestrian dynamics
Evacuation
Dynamic Monte Carlo
Cellular automata
Congestion

ABSTRACT

In this study, we investigate a two-dimensional lattice model for crowd evacuation dynamics by using a dynamic Monte Carlo (DMC) method. This model is built on the microscopic Arrhenius dynamics along with the exclusion rule in which stochastic processes govern the individual movements depending on the relative distance to the room exit. Even though individual decision-making procedures can be complicated during the evacuation in an emergency, our model can quantitatively estimate the time for them to evacuate and predict the emerging patterns of the crowds during the process. The results exhibit the phenomena such that pedestrians spontaneously gather at the exit and form an arched shape close to the door. The DMC simulations and observations agree with the corresponding study in the literature. The DMC algorithm is computationally efficient due to its major property —"rejection-free", which makes it a suitable tool to simulate evacuation dynamics for a large group of pedestrians.

© 2023 Elsevier Inc. All rights reserved.

1. Introduction

With the growth in urban population, there are increasing numbers of gathering events for living, working, studying, or entertainment. There have been incidents where overcrowded groups of people tried to evacuate in case of emergencies leading to injuries and casualties [1–3]. Despite the massive fatalities caused by these circumstances in the community, the dynamics of urgent evacuation are not comprehensively explored and investigated [4]. Emergency evacuation experiments in real life are challenging to conduct, in particular with humans, due to possible ethical and legal controversy. Therefore, the numerical study of pedestrian dynamics, especially evacuation processes, can provide valuable information for architectural design, facilities optimization, crowd management, and emergency planning, which can help to improve crowd safety. Researchers observe a number of self-organized phenomena and collective effects emerged in the pedestrian flow, for example, lane formation, jamming, clogging, zigzag, and faster-is-slower effect [5–10].

The models for describing pedestrian flows can be categorized into two major classes: macroscopic and microscopic models. The macroscopic ones treat crowds as a homogeneous mass that behaves like a compressible fluid flow. The density and the flux of pedestrians are related by using partial differential equations, specifically, in the theory of fluid dynamics and the conservation laws [11–14]. On the other hand, the microscopic models describe the dynamics of each pedestrian by incorporating the interactions between pedestrians and individual heterogeneity, such as age, gender, physical condition, and preference in moving directions.

E-mail addresses: ntamang@email.sc.edu (N. Tamang), yisun@math.sc.edu (Y. Sun).

^{*} Corresponding author.

The microscopic representations could be roughly divided further into continuous and discrete models. One popular example on the continuous microscopic level is the social-force model, which describes the motion of each pedestrian with their interactions based on the distances between them by using the ordinary differential equations (ODEs) [4,15–18]. The social-force model involves solving a high-dimensional system of ODEs for a large number of pedestrians. Although the system of equations can be solved with standard numerical integration schemes, the numerical solutions may highly oscillate and be unstable even by taking very small time steps [18]. In the discrete models, space is partitioned into small cells or lattice sites that the pedestrians stay in. At each step, an individual moves to one empty neighboring cell or site with certain probabilities. An example of the discrete models is the cellular automaton (CA) model [19–21], in which the movements of pedestrians are described by a number of rules that may depend on the exit location, the exit width, the distance to the exit and inherent characteristics such as gender and movement speed, and interactions with other pedestrians [22–27]. It is difficult to claim which class of models is more accurate than the other because the individuals neither act together as rigid bodies with regular shapes, nor behave in a uniform manner [28]. Both macroscopic and microscopic models can simulate typical patterns during the evacuation dynamics, including clogging and arching of pedestrians around an exit.

The update strategies for the CA models include two types: graph-based and field-based. In the graph-based models, pedestrians move towards one orientation point, steering towards the final target in a randomly determined sequence of events. The field-based models take account of other influences, such as the distance to an exit and infrastructure/obstacles in the room. These influences can be reflected as a static floor field, which does not change throughout a simulation. In [22,23], the so-called *floor field* model was introduced by Schadschneider and collaborators, which has become a standard CA approach to pedestrian dynamics.

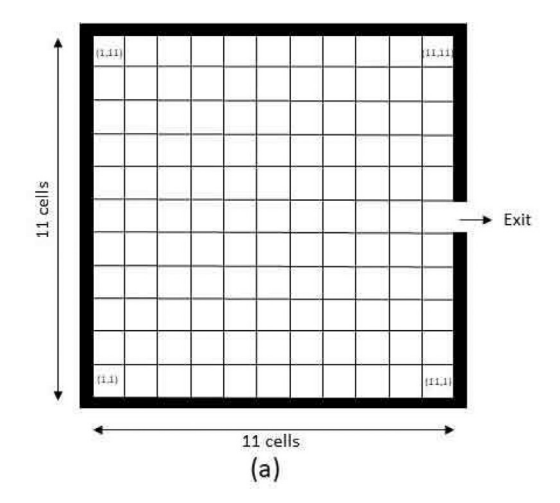
Recently, the CA models have been widely applied to simulate the evacuation dynamics due to their conceptual simplicity, and numerical efficiency [29]. Song et al. [30] and Cao et al. [31] developed a multi-grid model that takes finer lattice and each individual occupies several cells instead of one. Ren et al. [32] proposed a pedestrian evacuation model with multi-exits based on a force-driven CA. In [33], Lu et al. took an extended floor field CA model to study pedestrian group behaviors in crowd evacuation. Li et al. [34] proposed a CA model of pedestrian movements with a visibility function defined to describe the visual effect. Henein and White [35] took crowd forces and associated injuries into account in their CA evacuation model. Wang et al. [36] and Zheng et al. [37] included a panic factor in the CA model to study the psychological effect of pedestrians on the evacuation process. Yi et al. [38] simulated evacuation of crowds in case of stampedes, in which individuals choose to follow the majority or stay away from the stampedes. Kim et al. [39] and Zheng et al. [40] studied the effect of fire and smoke on evacuations by taking a fire and smoke floor field in the CA model. Tanimoto et al. [41], Bouzat and Kuperman [26], and Chen et al. [28] applied the game theory in the CA model to resolve the situations when several individuals try to occupy the same target cell.

Our main goal in this work is to present a CA model on two-dimensional (2D) lattices to simulate the evacuation process in a scenario where crowds try to escape from a room with one or two exits. In our model, a pedestrian moves into a vacant neighboring cell with a probability that depends on his/her surrounding neighborhood at the moment. The probability is governed by stochastic processes built on the microscopic Arrhenius law and the exclusion principle. These rules reflect the pedestrians' decisions of action that an individual avoids collisions with other pedestrians, and pedestrians choose scholastically to move towards the exit, stop to wait, and back step. With this model, we simulate the evacuation dynamics on 2D lattices with the individual preference to leave a room via the shortest path possible for minimum effort. The proposed model and many CA models for pedestrian and traffic dynamics are close to the Ising model for equilibrium systems. In fact, these models can be seen as the Ising model's extension to the non-equilibrium dynamics for pedestrian and traffic flows.

To evolve the dynamics of pedestrians on a microscopic level more efficiently, we employ the kinetic/dynamic Monte Carlo (DMC) method [42,43] because of its major property —"rejection-free". When starting a DMC simulation, we put all of pedestrians' possible moving events into a list. Then in each time step, we randomly choose an event from the list with a probability proportional to the rate of the event by using a fast search. After performing the configurational change for this event, we update the event list. No event will be rejected in this way so as to save computational cost compared with the Metropolis Monte Carlo (MMC) algorithm [44]. Currently, a lot of CA models for simulating pedestrian and vehicular dynamics employ the MMC method. However, it sometimes rejects trial steps due to small acceptance probability rates, for instance, when a system is close to the equilibrium. Based on this reason, we adopt the DMC method instead of the MMC to evolve the evacuation dynamics. We have recently applied the DMC method to simulate 1D/2D traffic and bi-direction pedestrian flows [45–49].

We note that DMC is usually used in the study of material sciences such as simulating chemical deposition, crystal surface growth, and surface diffusion. To our knowledge, this is the first study that uses DMC for efficient uncertainty prediction for the crowd evacuation process within the literature. The DMC method can be a good choice to the current models for studying evacuation dynamics.

The structure of the paper is as follows. We introduce the CA model and the pedestrian evacuation strategies in Section 2. Then, in Section 3, the DMC algorithm and the implementation is outlined. In Section 4 we demonstrate several sets of numerical results with different parameters of the model. Finally, Section 5 summarizes our work and suggests future extensions.



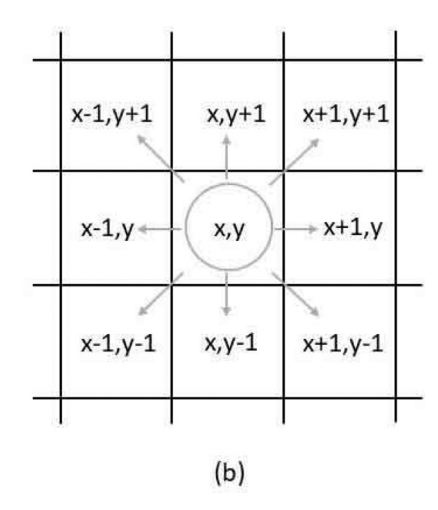


Fig. 1. (a) Schematic illustration of the $M \times M$ room with one exit of w cells wide on the east side (here, M = 11, w = 1. The exit is at the cell (12,6); pedestrians in three different cells (11,5), (11,6), (11,7) can exit the room; (b) The movement field of a pedestrian at the center, who can stay there or migrate into one of the neighboring sites.

2. A cellular automaton model

In this section, we present the 2D lattice (cellular automaton) model for evacuation dynamics, in which pedestrians try to reach their destination (i.e., the exit) while avoiding collisions with other individuals. A pedestrian chooses one of the empty neighboring lattice sites to move into based on the distance from the site to the destination. This distance determines the transition probability of the moving event. For simplicity, we consider a square room with one exit located at the center of one side of the square. The domain is divided into $M \times M$ cells or lattice sites, and M denotes the system size. One pedestrian can occupy only one site, and vice versa. The door width has w cells so that no more than w individuals could exit the room simultaneously (Fig. 1(a)). A pedestrian is considered as having exited the room when he/she moves into one of the exit cells. We characterize the state at every site (x, y) with an index $\phi_{(x, y)}$ $(1 \le x, y \le M)$:

$$\phi_{(x,y)} = \begin{cases} 1 & \text{if there is one person in the site } (x,y), \\ 0 & \text{if the site is vacant.} \end{cases}$$
 (1)

Then the system configuration is described by $\{\phi_{(x,y)}\}_{x,y=1}^{M}$ in the space $\{0,1\}^{M^2}$. Pedestrians' movements are described by the transitions between the system configurations. The pedestrians lie in the Moore neighborhood composed of eight nearest neighboring sites, as shown in Fig. 1(b). In each step, one individual is chosen to migrate into one of the eight neighboring sites if that site is empty [19]. These movements follow the spin-exchange dynamics [50]: the pedestrian's current site and the chosen neighboring site exchange their index numbers in each transition. For example, if a pedestrian occupying a site (x,y) migrates to a neighboring site (x',y'), the configuration is updated as follows:

$$\{\phi_{(x,y)} = 1, \ \phi_{(x',y')} = 0\} \rightarrow \{\phi_{(x,y)} = 0, \ \phi_{(x',y')} = 1\}.$$

In each step, a pedestrian selects his/her desirable site out of the eight neighboring sites based on the distances from these sites to the exit. In particular, the pedestrian is more likely to choose one of the vacant sites that is the closest to the exit. The pedestrians' movements are governed by the transition probabilities that depend on spatial one-sided interactions and the surrounding neighborhood. Here, we take an Arrhenius type interaction relation [51] and perform an individual movement with the transition rate defined by:

$$r = \omega_0 \exp\left(-E\right). \tag{2}$$

Specifically, a likelihood that a pedestrian occupying the site (x, y) moves to a neighboring site (x', y') follows

$$r_{(x,y)}^{(x',y')} = \omega_0 \exp\left(-\Delta d_{(x,y)}^{(x',y')} - \sqrt{2}\right),$$
 (3)

where the parameter $\omega_0=1/\tau_0$ denotes the pedestrian moving speed or frequency with τ_0 as the characteristic time. The term $\Delta d_{(x,y)}^{(x',y')}$ is given by

$$\Delta d_{(x,y)}^{(x',y')} = \sqrt{(x'-x_{\rm ex})^2 + (y'-y_{\rm ex})^2} - \sqrt{(x-x_{\rm ex})^2 + (y-y_{\rm ex})^2},\tag{4}$$

where (x_{ex}, y_{ex}) denotes the coordinates at the middle of the exit. The first term on the right hand side of Eq. (4) stands for the shortest distance from the neighboring site (x', y') to the exit, and the second term is the distance from the current

location (x,y) to the exit. As the values of Δd for all pedestrians' possible movements in one step are in the range of $-\sqrt{2}$ to $\sqrt{2}$, we normalize the exponent by subtracting with $\sqrt{2}$ so that the exponent is below or equal to 0 and the rate r is at most ω_0 . The transition probability for each pedestrian is computed according to his/her proximity to the exit and the Eq. (4) is inspired from Chen et al. [52]. Based on the Eqs. (3)-(4), we can see that among the eight neighboring sites around a pedestrian, the closer is the distance from the neighboring site (x',y') to the exit, the greater is the transition value r. If another agent already occupies the neighboring cell (x',y'), the rate $r_{(x,y)}^{(x',y')}=0$ due to the assumption that only one pedestrian can occupy one cell.

3. The dynamic Monte Carlo method

We evolve the CA model discussed above by using the dynamic Monte Carlo (DMC) algorithm since it has several advantages over the Metropolis Monte Carlo (MMC) method [44]. The first reason is that the selected events in the MMC method can sometimes be rejected if the acceptance rate is low, especially when the pedestrian density is large or the system is close to the equilibrium. The DMC algorithm with the key feature of being "rejection-free" was originally developed in [42] to speed up the MMC simulation of Ising models. Another reason to use the DMC method is its suitability and efficiency for simulating the non-equilibrium system due to the way how the transition rates are updated locally. For every time step, as the transition probabilities for all possible changes from the current state have been computed and stored in a list, we can select a transition event from the list by using a probability proportional to the corresponding event rate. To perform the event, only the information from two adjacent sites is swapped. Therefore, only a small number of individuals (if there are any) in the nearby neighboring sites need to be updated with their possible moving events in the list affected by the preceding event.

When applying the DMC algorithm, we usually assume that the system takes N independent processes (i.e., the pedestrian moving events) associated with the rates r_i given in Eq. (3), and these processes/events are of the Poisson process type. Then the DMC algorithm can give the correct time scale for the evolution of the system, which depends on the total rate given by the sum of all transition rates: $R = \sum_{i=1}^{N} r_i$. In each round of the DMC algorithm, we perform the following steps: The DMC algorithm

Step 1. Generate a random number $\xi_1 \in (0,1)$ from a uniform distribution. Decide which event will happen (i.e. which pedestrian and his/her moving direction) by selecting the event s such that

$$\sum_{i=1}^{s-1} \frac{r_i}{R} < \xi_1 \le \sum_{l=1}^{s} \frac{r_i}{R} \tag{5}$$

- Step 2. Update the configuration by executing the chosen event s.
- Step 3. Determine the time duration for the chosen event to take place (i.e., the transition time) by using R and another uniform random number $\xi_2 \in (0,1)$ to compute the nonuniform time step $\Delta t = -\ln(\xi_2)/R$.
- Step 4. Update any transition rates r_i and the total rate R that may have changed caused by the event, such as a pedestrian reaches the exit and leaves the room, a neighboring site changes from occupied to empty due to a pedestrian moving out of it, or vice verse.
 - **Remark 1.** When we select an event in Step 1, instead of doing a naive linear search with O(N) operations, we should use a binary search that can bring down the searching cost to $O(\log_2 N)$ operations.
 - **Remark 2.** We repeat the above Steps 1 to 4 until the last pedestrian leaves the room as the DMC simulation procedure is finished. The total time that it takes for all pedestrians to exit the room is referred as the evacuation time.

4. Numerical experiments

In this section, we investigate the evacuation dynamics with various parameters using the DMC algorithm presented in the previous section. Following [8,46,53,54], we take the actual physical cell-size as $0.4 \times 0.4 \text{m}^2$ in order to allocate enough space for everyone to maintain a safe distance to others and avoid bumping into them. This assumption agrees with the observation that the highest density in dense crowds is roughly 6 peds/m². We first focus on the situation that the evacuation is performed in a square room with an exit located in the middle of the east side, as shown in Fig. 1(a). At the beginning, total N_p pedestrians are randomly distributed in the room, hence the initial population density (i.e., the occupancy rate) $\rho = N_p/M^2$ with $0 \le \rho \le 1$. As the evacuation starts, all pedestrians move towards the exit at the desired velocity of 1.2 meters per second (i.e., 3 cells per second). This speed can be set by imposing the characteristic time $\tau_0 = 1/3$ s, and then $\omega_0 = 3\text{s}^{-1}$. Actually, pedestrians sometimes might move slower or faster than the average speed because of the inherent stochasticity in the system.

4.1. Comparisons between different population densities

Our first set of experiments aim to compare the results of different densities ρ with a fixed room size M=30 cells (= 12m) and an exit of the width w=1 cell (= 0.4m). Figure 2 illustrates six typical snapshots at different times of a

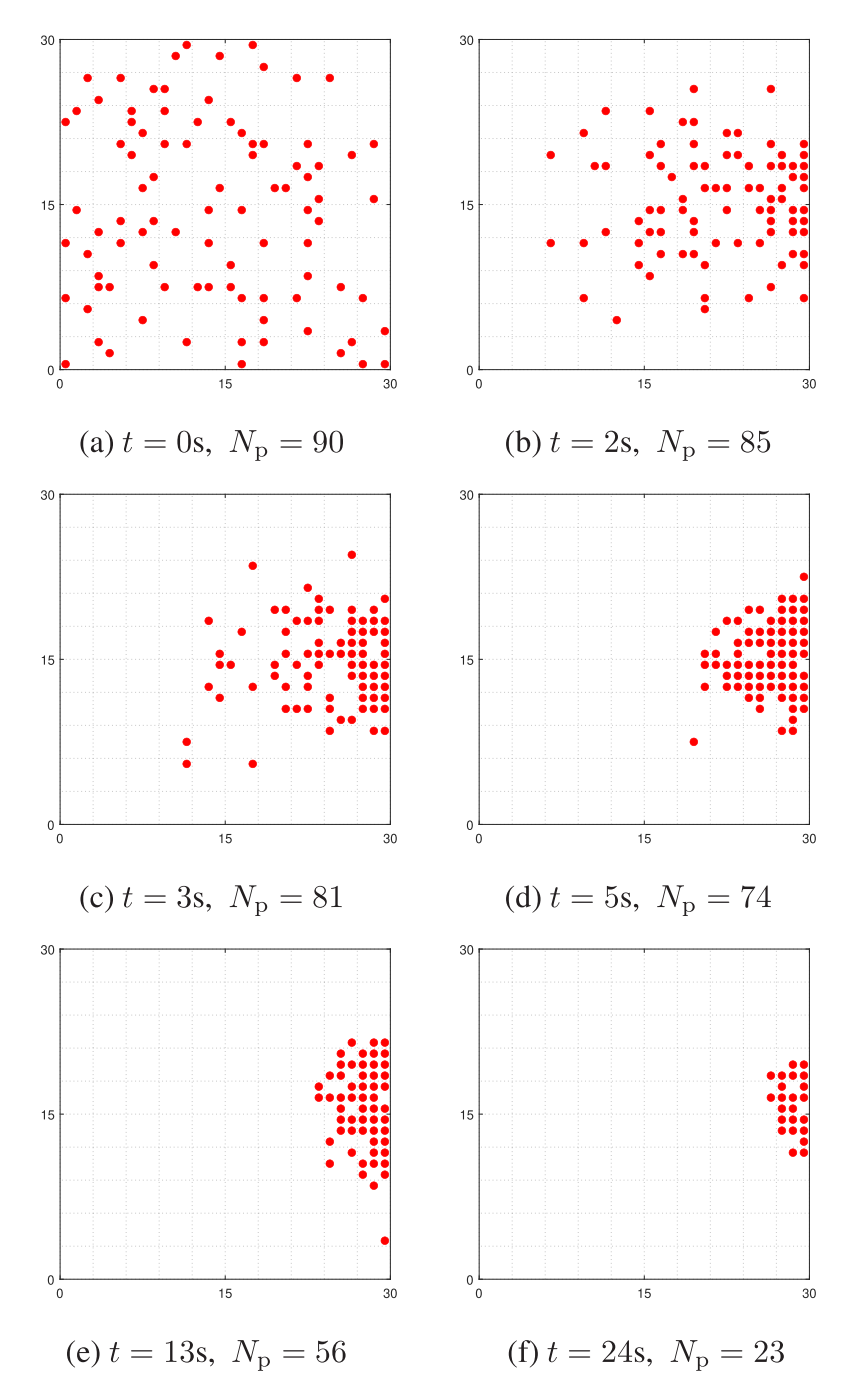


Fig. 2. Six snapshots of a DMC simulation for the pedestrian evacuation from a room of size M = 30. The initial density $\rho = 0.1$, so the initial number of pedestrians $N_p = 90$.

DMC simulation. Initially, $N_p = 90$ pedestrians (as $\rho = 0.1$) are distributed randomly inside the room with the exit at the site (31,15) (Fig. 2(a)). Once the evacuation starts, all pedestrians move by trying to follow their shortest paths to the exit (Fig. 2(b)–(d)). At t = 13s (Fig. 2(e)), more than 1/3 of total pedestrians have already moved out of the room while most of the remaining pedestrians are clogging in front of the door. At t = 24s (Fig. 2(f)), about 1/4 of total pedestrians are still inside the room. By the time $t \approx 33$ s, all of pedestrians have evacuated from the room (the configuration not shown).

Figure 3 shows another DMC simulation for the evacuation process of total $N_p = 360$ pedestrians (as $\rho = 0.4$) from the same room with the same exit location. It takes much longer time for all pedestrians to leave the room; however, similar

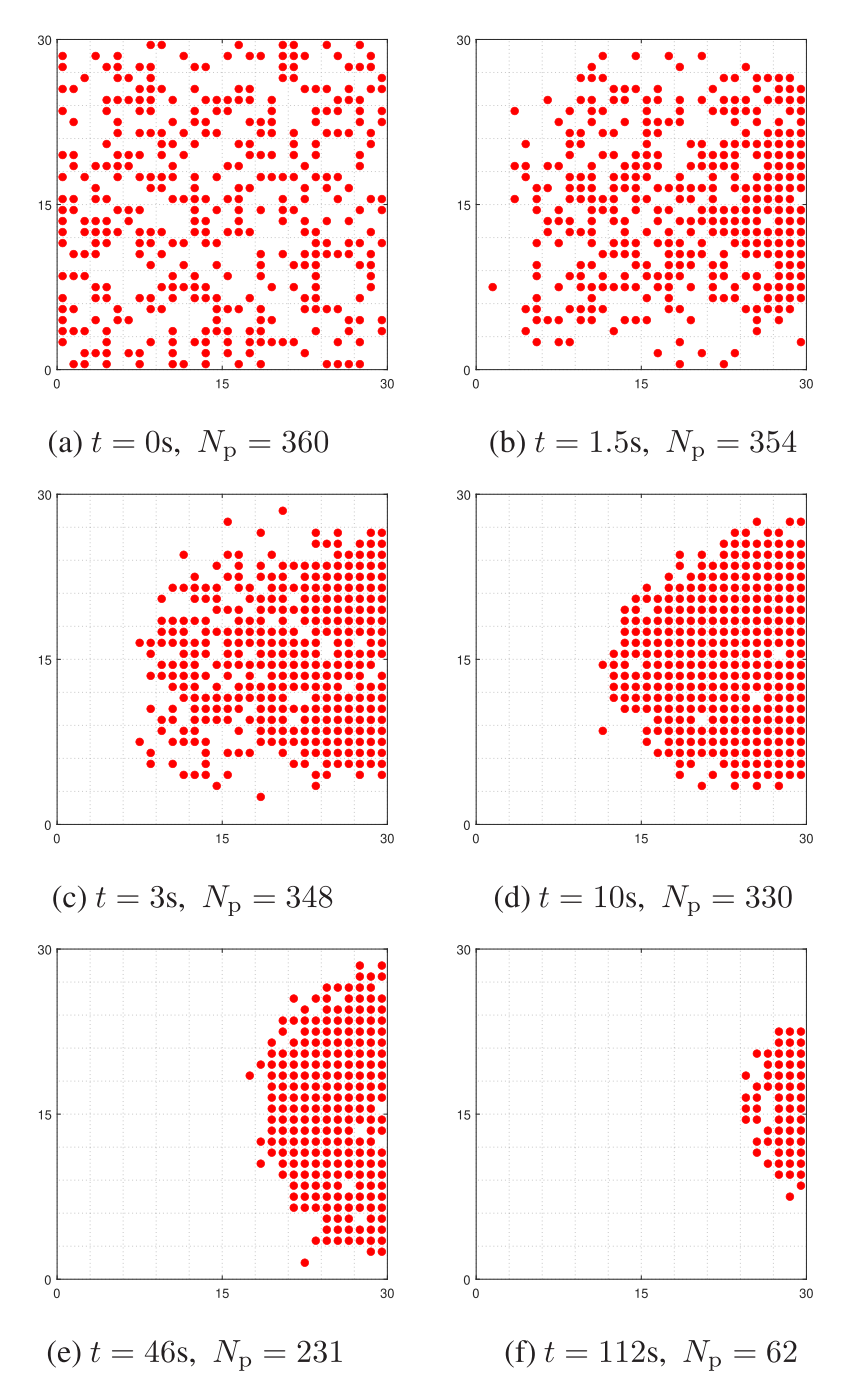


Fig. 3. Six snapshots of a DMC simulation for the pedestrian evacuation from a room of size M = 30. The initial density $\rho = 0.4$, so the initial number of pedestrians $N_p = 360$.

behaviors and patterns can be observed here. Many pedestrians gather in front of the exit due to its limited width. In particular, at time t = 46s (Fig. 3(e)), the remaining pedestrians form a semi-elliptic shape (an arching) in front of the door. The update rule in Eqs. (3)-(4) implies that the pedestrians during an evacuation process will perform a biased random walk as they will choose the direction towards the exit with the highest probability. The typical patterns of the evacuation dynamics have been observed in Figs. 2 and 3, and other simulations. In summary, the typical patterns are the following: (i) At the beginning, individuals are randomly distributed. (ii) As individuals move to the exit, the crowd gathers around the exit and becomes denser and denser, which forms an arching and clogging due to the inefficient and irregular outflow. (iii)

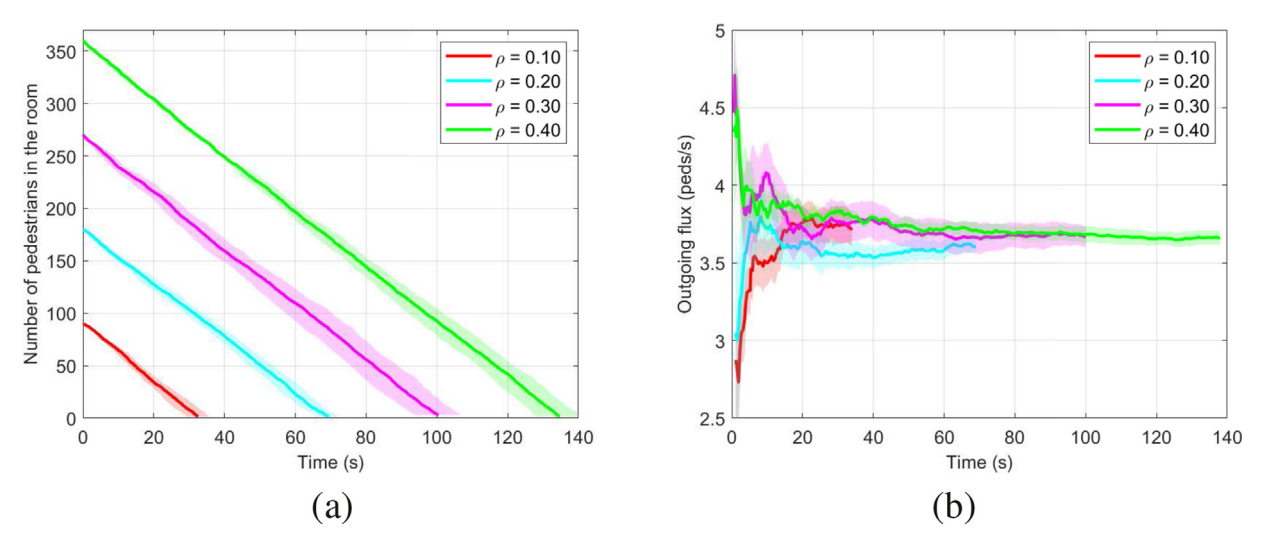


Fig. 4. (a) Comparison of the number of remaining pedestrians in the room versus time with four different initial density ρ from 0.1 to 0.4. (b) The averaged outgoing flux versus time. We take the same room size M=30 cells and the same exit width w=1 site in all DMC simulations. For each initial density ρ , we present the averaged result over ten simulations with different random number seeds. The shaded area depicts the mean \pm the standard deviation.

As more pedestrians exit the room, the size of the dense crowd decreases. (iv) Finally, the crowd disappears, and it reaches the end stage of the evacuation.

Figure 4(a) shows the evolution of the number of individuals remaining in the room and the comparison between the results of different initial population density ρ from 0.1 to 0.4. Here we set the same room size (M=30) and the same exit width (w=1) in all DMC simulations. Furthermore, for each initial density ρ , we run ten simulations with different random number seeds and show the averaged results. For a given value of ρ , all pedestrians are able to successfully evacuate from the room, and the number of remaining pedestrians decays almost linearly in time. The average evacuation time for the initial density ρ from 0.1 to 0.4 is approximately 33s, 68s, 101s, and 135s, respectively. We observe that the evacuation time increases almost linearly as ρ increases.

Meanwhile, Fig. 4(b) shows another quantity of interest, the outgoing flux over time, i.e., the average number of individuals exiting the room per unit of time [57]. At the beginning, the outgoing fluxes of $\rho=0.1$ (red) and $\rho=0.2$ (cyan) increase while the ones of $\rho=0.3$ (pink) and $\rho=0.4$ (green) decrease. After certain transient periods, all outgoing fluxes become uniform over time and approach to about $3.6\sim3.7$ pedestrians per second. One possible cause for these transients is that the individuals initially close to the door can exit the room before the rest pedestrians start clogging and form an arching by the exit. If the initial density is low, it takes time for individuals to walk to the door before they exit, therefore the initial outgoing flux is small. On the other hand, if the initial density is high, more individuals are close to the exit so that more people can exit the room within the same time frame at the beginning. After the transient period, the outgoing flux becomes essentially uniform over time regardless of the initial density because the width of the exit limits the flow of pedestrians.

4.2. Comparisons between different exit widths

Next, in the second set of experiments, we study the effect of the exit width w on the evacuation time in Fig. 5. Here we generate random initial distributions with the population density increasing from $\rho=0.05$ to $\rho=0.95$ and compare the evacuation times for four different exit widths from w=1 cell (= 0.4m) to w=4 cells (= 1.6m). But we keep the same room size M=30 cells (= 12m) in all DMC simulations. Again, we show the averaged result for each value of ρ over ten different simulations. In Fig. 5, we observe that the average evacuation time for a given door width increases linearly with the initial density ρ . The pedestrians gather around the exit after the evacuation process starts; however, the rate at which the pedestrians evacuate is limited by the size of the door. Furthermore, for each density ρ , we observe that the time it takes for all pedestrians to evacuate is the longest for the case with the door width w=1, and the average evacuation time decreases when we widen the exit as expected. In particular, the fitting lines in Fig. 5 show that the case with w=1 has the largest slope, which is much steeper than the other three cases. Indeed, for the simulations with w=1, we observe that the pedestrians always gather around the door and clog the exit in the majority of the simulations, which produces a much longer evacuation time. Therefore, by having a larger exit, multiple pedestrians are able to exit the room at the same time, which can reduce the evacuation time.

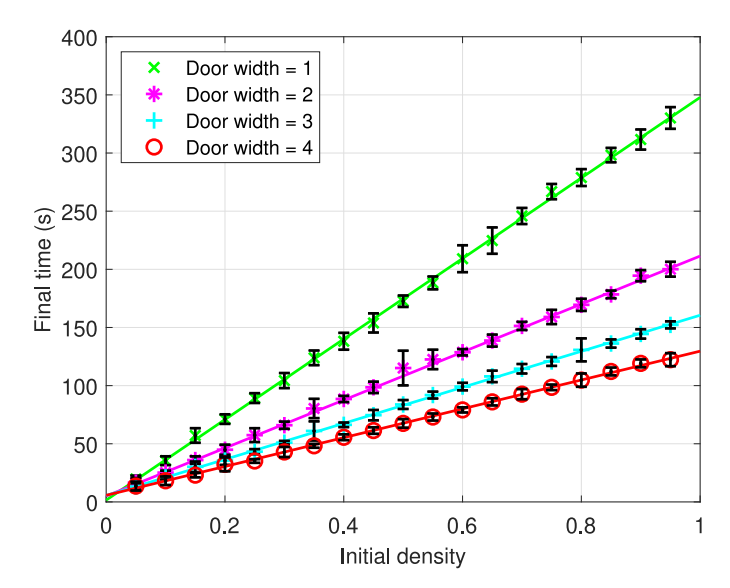


Fig. 5. Comparison of the evacuation time versus the initial density ρ with four different exit widths w from 1 to 4 sites. We take the same room size M=30 in all DMC simulations. For each initial density ρ , we present the averaged result over ten different simulations. The error bars are the mean \pm the standard deviation. The solid lines from top to bottom are (1) $t_{\rm ev}=1.54+346.31\rho$, (2) $t_{\rm ev}=5.03+206.39\rho$, (3) $t_{\rm ev}=5.55+154.98\rho$, and (4) $t_{\rm ev}=5.70+123.93\rho$, respectively, where $t_{\rm ev}$ represents the evacuation time and ρ is the initial population density.

To understand the intermediate stage during the evacuation, we also consider the distribution of time intervals between successive pedestrians passing through the door. Figure 6 shows the histogram of time intervals Δt between successive exit times, collected from ten simulations of evacuations at the initial density of $\rho=0.5$ from a room of size M=50 with a door width of w=1 to 4 cells, respectively. The histograms shown in Fig. 6(a)-(d) are right-skewed, and increasing the door width can reduce the median of the time intervals Δt . The appearance of events with larger Δt indicates that there are temporary cloggings during the evacuation process. In the histograms, the range of possible clogged time of the case with w=1 is much broader than those of the other three cases. Figure 6(e) compares the distributions of Δt collected from ten simulations with four different door widths on a semi-log scale. Although these distributions are not identical, the frequency appears to be an exponential decay with Δt across the four different sizes of the door shown by linear behavior on a semi-log plot.

4.3. Comparisons between different room sizes

Emergency evacuation could arise in various spatial sizes, from a number of customers in a bar to a large crowd in a packed concert hall. Here, the third set of experiments aim to the effect of the room size M on the evacuation dynamics. In Fig. 7, we run five sets of DMC simulations to compare the evacuation times for different room sizes from M=10 cells (= 4m) to 50 cells (= 20m). But we keep the same exit width w=1 cell (= 0.4m) in all simulations. Similar to the previous discussion in Sections 4.1 and 4.2, we observe that for each room size M, the evacuation time is approximately a linear function of the initial density ρ . For the same initial density ρ , the evacuation time for the larger room size M is longer as there are more pedestrians than in the smaller room. For these almost linear functions, the slope of the one for the larger room appears to be steeper since the initial number of pedestrians is proportional to the square of the room size, i.e., M^2 .

4.4. Comparisons to relevant previous work

Here, in the fourth set of experiments, we show the comparison between our DMC simulations and the ones from other models reported in Refs. [15,55] in three scenarios with different room sizes, door sizes, initial numbers of pedestrians, and velocities. In the typical scenario when pedestrians evacuate from a single-door room, all of the simulations and the reported results demonstrate a clogging effect and an arching effect near the exit due to the limitation of the door width. Table 1 shows the evacuation times obtained from our models with the ones from the social force model [15] and the lattice gas model [55]. The reported evacuation time is approximated from the figures shown in the references, and the DMC results are the averaged evacuation times over ten simulations with their standard deviations. The table indicates the agreement between the predicted evacuation time using the DMC method and the ones reported in the previous studies.

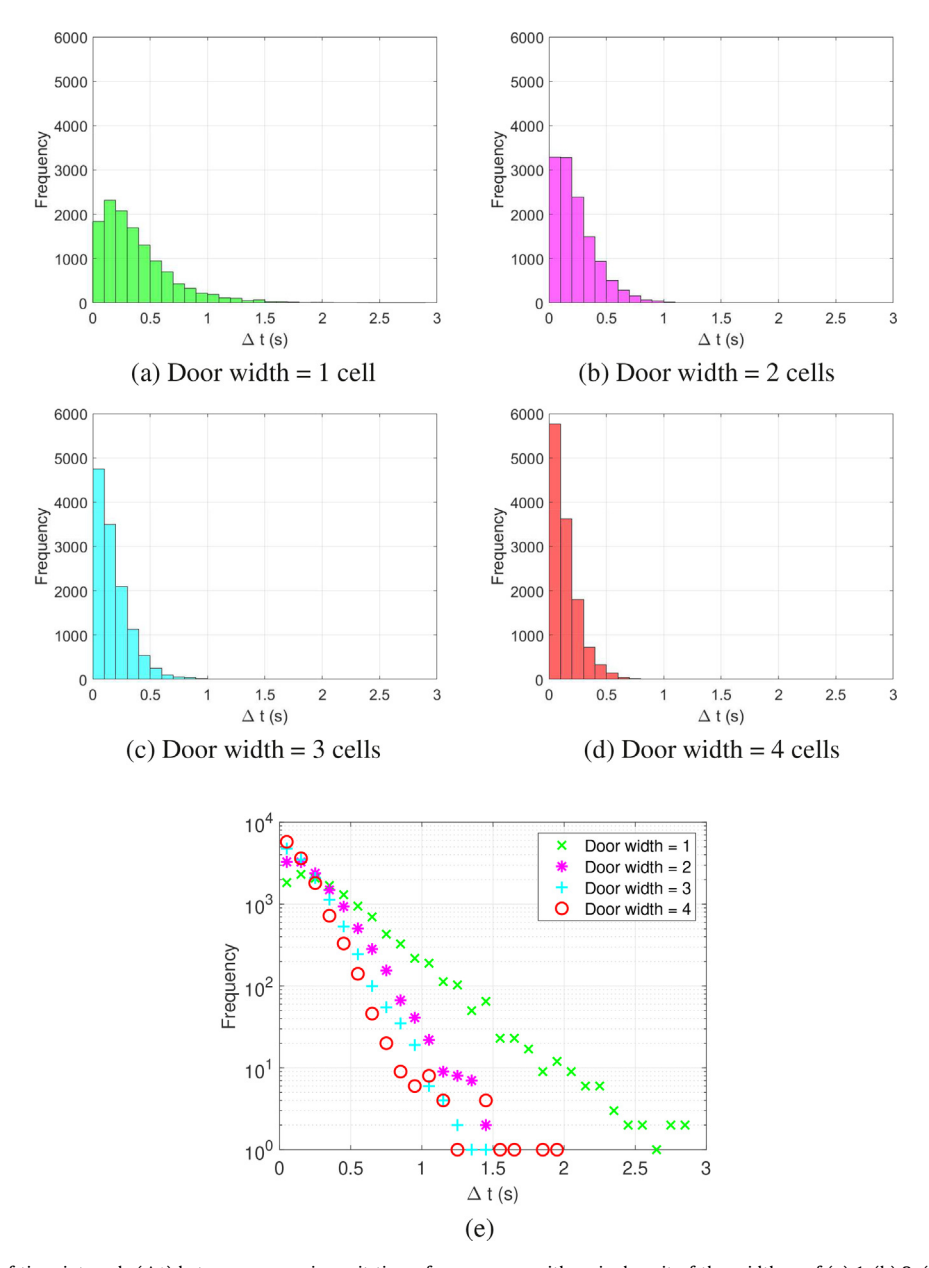


Fig. 6. Histograms of time intervals (Δt) between successive exit times from a room with a single exit of the width w of (a) 1, (b) 2, (c) 3, and (d) 4 cells, respectively. The bin size of the histogram takes 0.1s. The panel (e) plots the frequency of the four sets of data in a semi-log scale. Each set of data is accumulated from ten simulations with M=50 and $\rho=0.5$.

Table 1Comparison results of the evacuation times in different scenarios obtained by our models with the results from other models in the literature. Note that the sign "≈" is used for the results by other models since these data are extracted from the figures shown in Refs. [15,55]. Our results are the averaged evacuation times over ten simulations with their standard deviations.

	Room size (cell ²)	Door width	Initial number	Velocity (m/s)	Evacuation time (s)
Ref. [55]	30 × 30	0.8 m	100 peds.	1.0	≈ 27.4
DMC results	30 × 30	2 cells	100 peds.	1.0	27.42 ± 1.18
Ref. [55]	30 × 30	0.8 m	100 peds.	1.33	≈ 25.2
DMC results	30 × 30	2 cells	100 peds.	1.33	24.73 ± 1.07
Ref. [15]	50 × 50	1.2 m	225 peds.	1.0	≈ 48.4
DMC results	50×50	3 cells	225 peds.	1.0	52.37 ± 2.73

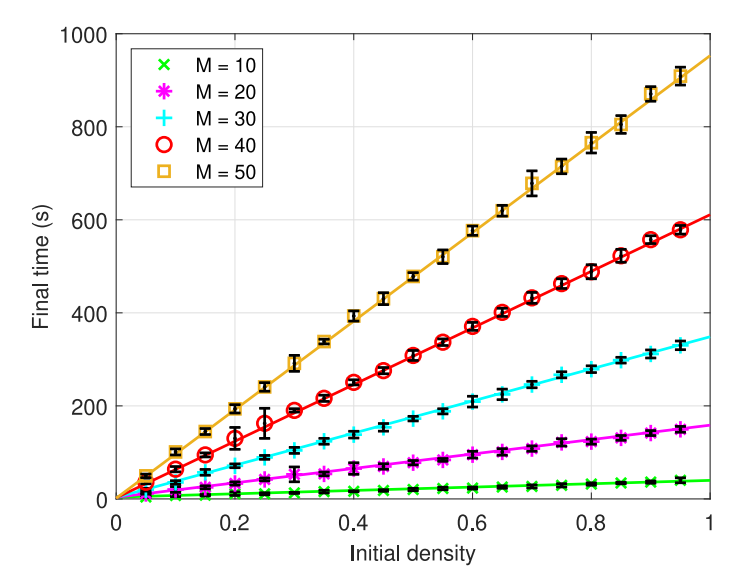


Fig. 7. Comparison of the evacuation time versus the initial density ρ with five different room sizes M from 10 to 50. We set the exit width w=1 cell in all DMC simulations. The results are averaged over ten different simulations for each value of ρ and M. The error bars are the mean \pm the standard deviation. The solid lines from top to bottom are (1) $t_{\rm ev}=1.54+951.42\rho$, (2) $t_{\rm ev}=2.26+608.74\rho$, (3) $t_{\rm ev}=3.29+345.31\rho$, (4) $t_{\rm ev}=3.55+154.98\rho$, and (5) $t_{\rm ev}=3.79+36.04\rho$, where $t_{\rm ev}$ represents the evacuation time and ρ is the initial population density.

4.5. Numerical simulation of evacuation with two exits

In the fifth set of experiments, we extend the evacuation model to a room with two exits. Once the evacuation starts, every pedestrian chooses his/her desired exit based on the shortest distance from his/her location to the exit. Then all pedestrians move towards their chosen exits.

Figure 8 shows six typical snapshots at different times of a DMC simulation. Initially, $N_p = 360$ pedestrians (as $\rho = 0.4$) are distributed randomly inside the room with one exit of the width w = 1 cell placed at the center of the west side, (0,15), and the other exit located at the center of the east side, (31,15) (Fig. 8(a)). Since pedestrians choose the closest exit based on their proximity to the door, the room is divided into two sub-areas. The pedestrians represented by blue (\blacktriangleleft) in the left part prefer to take the west exit, while the others denoted by red (\blacktriangleright) in the right part choose the east exit. Each group has about 180 individuals. After the evacuation starts, all pedestrians move by trying to follow their shortest paths to their preferred exits (Fig. 8(b)–(d)). As only one person can exit through the door at any time, pedestrians start to form an arching at each exit (Fig. 8(d)). The size of the arching declines as more pedestrians exit the room (Fig. 8(e)–(f)). By the time $t \approx 28$ s, all of pedestrians have evacuated from the room (the configuration not shown).

In Fig. 9(a), we show the average and variance of the number of individuals remaining in the room over time from ten simulations and compare the results of different initial population density ρ from 0.1 to 0.4. Here we set the same room size (M=30) and the same exit width (w=1) in all DMC simulations. The number of remaining pedestrians decays almost linearly in time. The average evacuation time for the initial density ρ from 0.1 to 0.4 is approximately 7.5s, 15s, 22s, and 28s, respectively. We observe that the evacuation time increases almost linearly as ρ increases. Comparing to Fig. 4(a) of the results with only one door, the evacuation time in Fig. 9(a) is reduced by more than a factor of four. This might result from the additional exit and the reduction of the maximum distance that an individual has to travel to the exit.

Figure 9(b) shows the outgoing rate at which individuals exit from the two doors over time. At the beginning, the outgoing fluxes increase for all cases of $\rho = 0.1$ to 0.4. After certain transient periods, all outgoing fluxes become essentially uniform over time and approach to the values between $10.0 \sim 10.5$ pedestrians per second.

4.6. Comparisons between different exit locations

In the last set of experiments, we consider the effects of the exit locations on the evacuation process. In one case, there are two exits located in the middle of the north and east sides of a square room. In the other case of a rectangular room, two exits are located on the north and east sides, but the one on the north side is off-centered.

Figure 10 shows six typical snapshots at different times of a DMC simulation for the first case. Initially, $N_p = 360$ pedestrians (as $\rho = 0.4$) are distributed randomly inside the room with one exit of the width w = 1 cell placed at the center of the north side, (15,31), and the other exit located at the center of the east side, (31,15) (Fig. 10(a)). Similar to the case in the previous section, the pedestrians are separated into two groups based on their proximity to the exits. The pedestrians

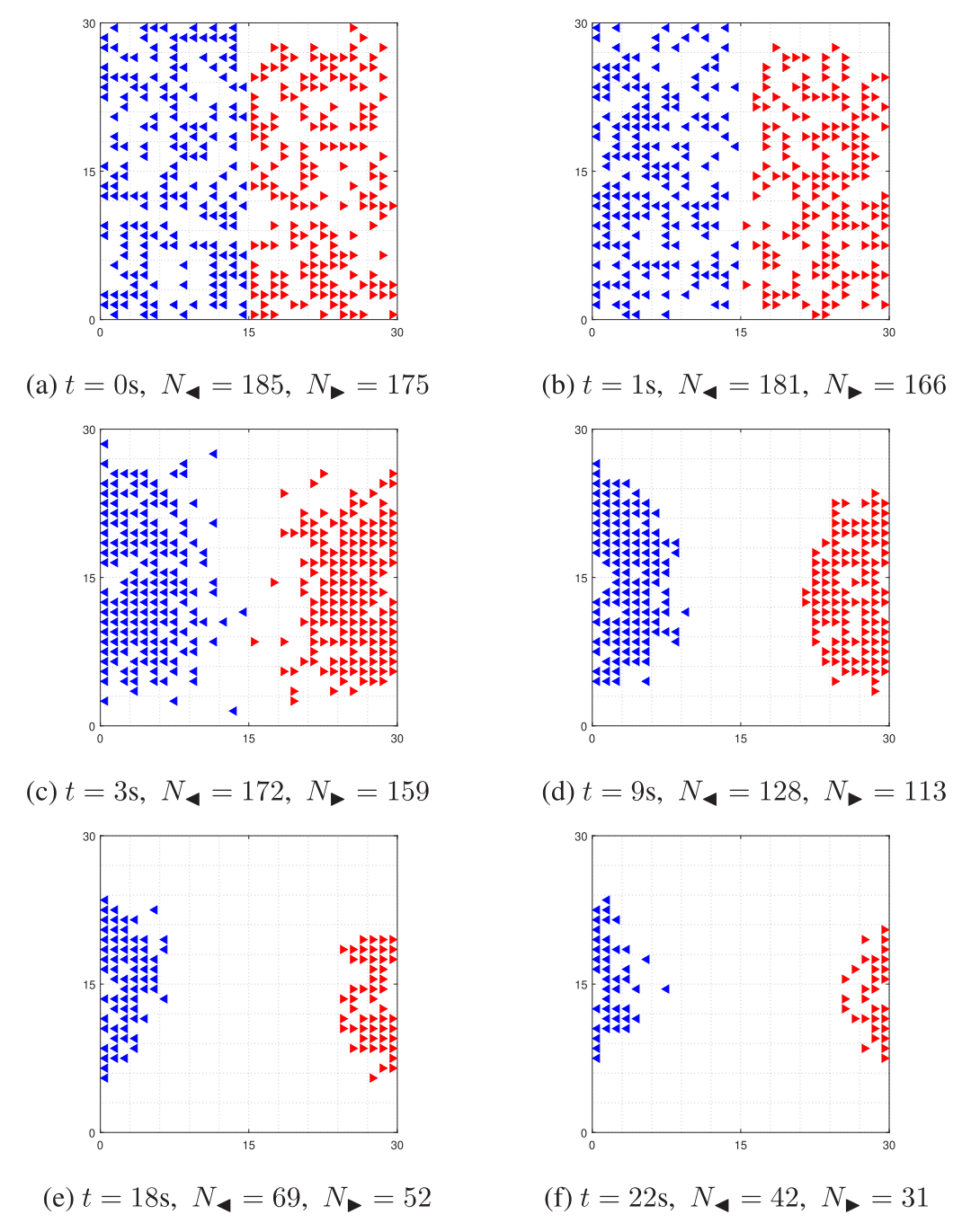
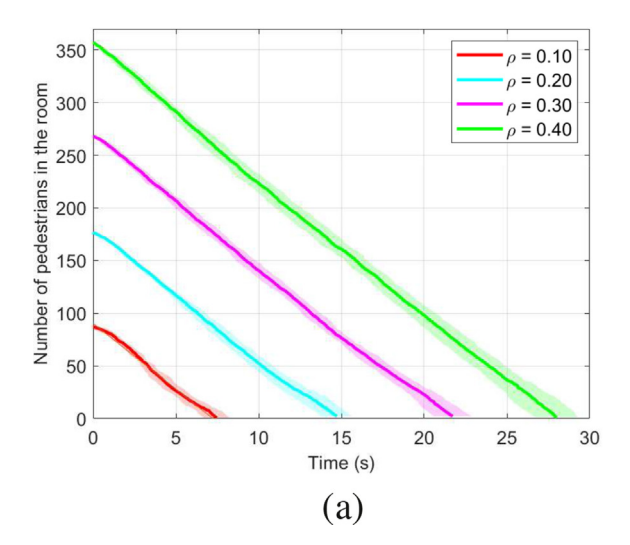


Fig. 8. Six snapshots of a DMC simulation for the pedestrian evacuation from a room of size M = 30. The initial density $\rho = 0.4$, so the number of pedestrians $N_p = 360$. The two doors are located in the middle of the west and east sides of the room, i.e. (0,15) and (31,15).

represented by black (\blacktriangle) prefer to take the north exit, while the others denoted by red (\blacktriangleright) choose the east exit. Each group has about 180 individuals. As all pedestrians move towards their preferred exits, the crowds gather around the exits waiting to escape from the room. The crowds decrease in size as pedestrians continuously exit the room (Fig. 10(b)-(f)). By the time $t \approx 30$ s, all of pedestrians have evacuated from the room (the configuration not shown).

The second case simulates an evacuation from a rectangular room with the size of 50×30 cells. Two doors of the width w=1 cell are located at (6,31) on the north side and (51,15) on the east side, respectively. Figure 11 shows six typical snapshots at different times of a DMC simulation for the second case. Initially, there are $N_p=600$ pedestrians (as $\rho=0.4$)



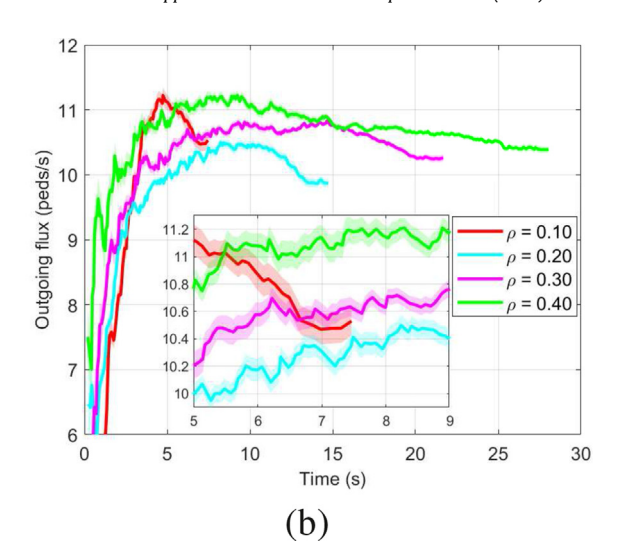


Fig. 9. (a) Comparison of the number of remaining pedestrians in the room versus time with four different initial density ρ from 0.1 to 0.4. (b) The averaged outgoing flux versus time. In all DMC simulations, we take the same room size M=30 cells, and there are two doors with the width (w=1 cell) located in the middle of the east and west sides of the room. For each initial density ρ , we present the averaged value over ten different simulations. The shaded area depicts the mean \pm the standard deviation. The inset in (b) zooms in the results to show the standard deviation.

distributed randomly inside the room (Fig. 11(a)). Again, the pedestrians are separated into two groups based on their preference of the exits. Each group has about 300 individuals. Once the evacuation starts, they move towards the closer exit and form an arching around each exit (Fig. 11(d)). By the time $t \approx 63$ s, all of pedestrians have evacuated from the room (the configuration not shown).

Figure 12 shows the evolution of the number of individuals remaining in the room for the two cases. For each case, we run ten simulations with different random number seeds and show the averaged results. The black and red lines correspond to the number of individuals who choose the north and east exits, respectively. In Fig. 12(a) of the first case with the square room, we observed that the black and red lines almost overlap with each other due to the symmetry of the locations of the two exits.

On the other hand, Fig. 12(b) of the second case with the rectangular room shows some difference between two groups. Although each group initially has about the same of 300 individuals, the group of pedestrians walking to the north door take more time (about 3 s) to exit the room. One possible reason may be due to the location of the north exit at (6,31), which is very close to the wall x = 0 (Fig. 11(a)). Therefore, the majority of pedestrians in this group (black \blacktriangle) are initially distributed to the east of the line x = 6. Once this group of pedestrians are clogging to form an arching (Fig. 11(d)), it is not centered at (6,31). Due to this biased distribution, they need to wait more time to exit. When the other group of pedestrians (red \blacktriangleright) are clogging, the formed arching is centered at (51,15), which is in the middle of the east side. Due to the symmetric distribution, this group may take relatively less time to exit.

4.7. Limitations and future improvements

Overall, the CA model with the DMC method presented in this study describes the movements of pedestrians well. The model can reproduce some collective phenomena like clogging at exit doors. While the DMC method can be viewed as a promising alternative to existing stochastic simulation tools for CA models of pedestrian or vehicular flows, there are some issues about our CA model that need to be considered.

The model contains free parameters such as the speed of individuals that can be calibrated to fit different quantitative descriptions of pedestrians. However, the parameters depend on the scenario and geometry of the domain, like long corridors, bottlenecks, and outflow from a room. The DMC transition rates can also be time-dependent and location-dependent instead of a constant. Therefore, they need to be calibrated with specific applications to make the prediction more reliable. In this study, we restrict the simulations to some simple scenarios, i.e., evacuation from a square or rectangular room with one or two exits. Here, our model uses the proximity to the exit to compute the transition rates for pedestrians' movements. The model can be improved further by considering pedestrians with different characteristics such as walking speeds and competitiveness.

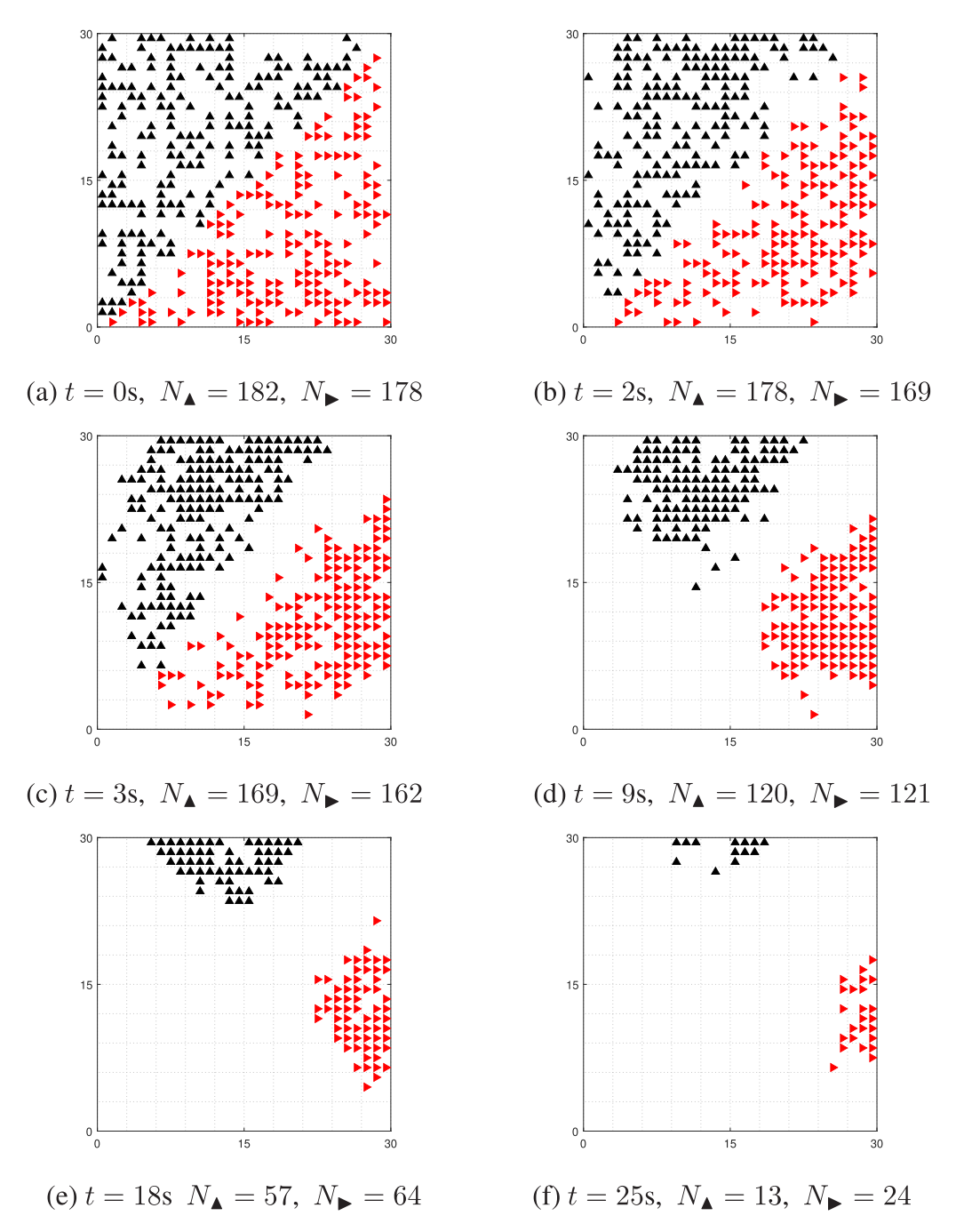


Fig. 10. Six snapshots of a DMC simulation for the pedestrian evacuation from a room of size M = 30. The initial density $\rho = 0.4$, so the number of pedestrians $N_p = 360$. The two doors are located in the middle of the north and east sides of the room, i.e. (15,31) and (31,15).

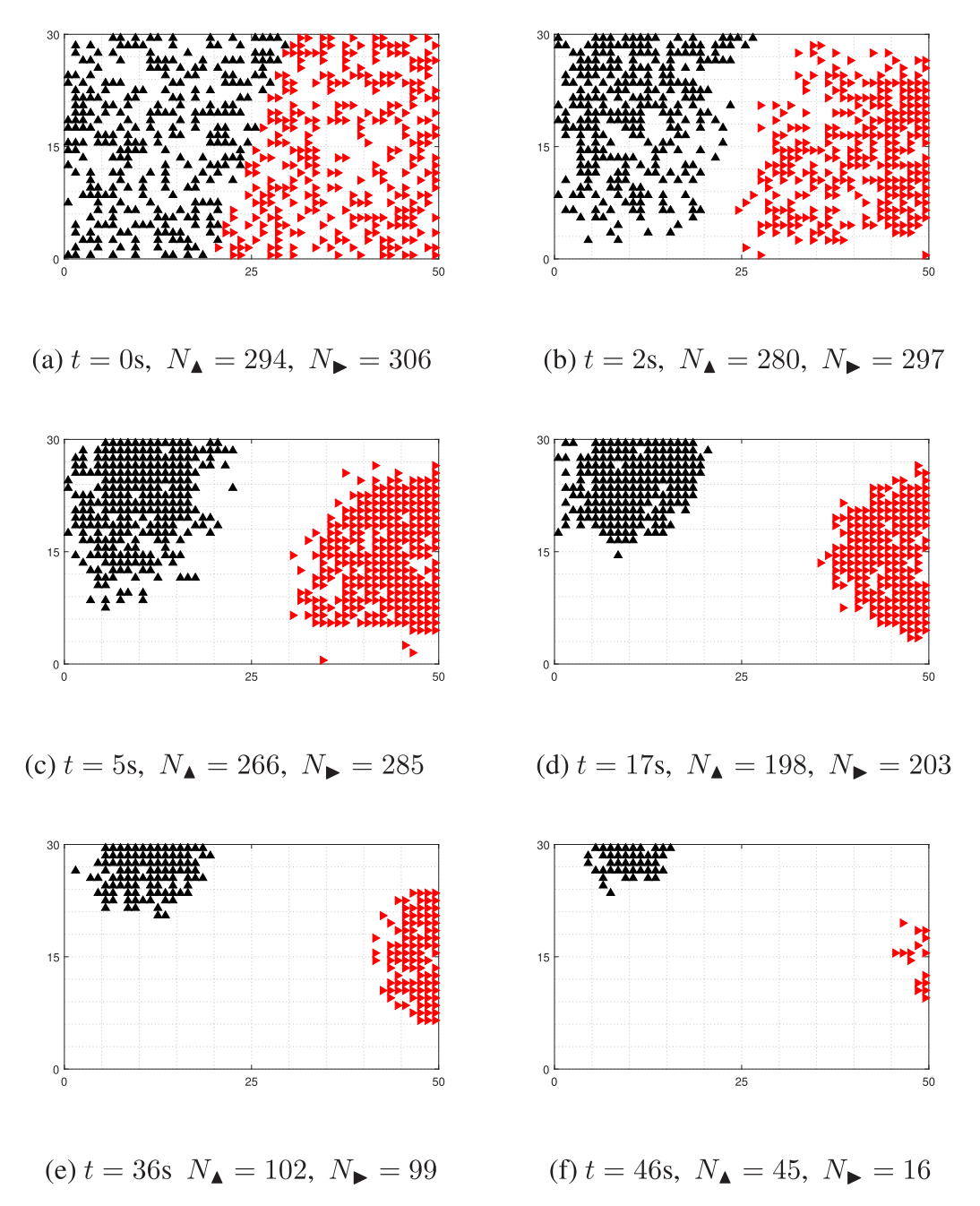
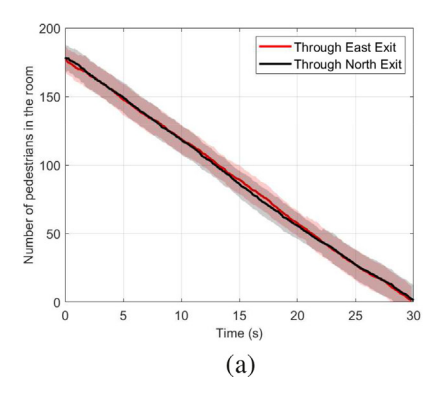


Fig. 11. Six snapshots of a DMC simulation for the pedestrian evacuation from a room of size 50×30 . The initial density $\rho = 0.4$, so the number of pedestrians $N_p = 600$. The two doors are located at (6,31) on the north side and (51,15) on the east side.



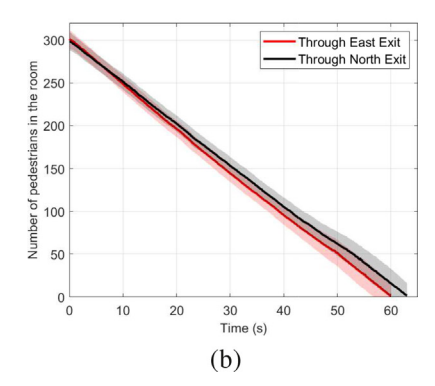


Fig. 12. Comparison of the number of remaining pedestrians in the room versus time with the initial density $\rho = 0.4$. (a) The case of the square room; (b) The case of the rectangular room. For each case, we present the averaged result over ten simulations with different random number seeds. The shaded area depicts the mean \pm the standard deviation. The black and red lines correspond to the number of individuals who choose the north and east exits, respectively. (For interpretation of the references to colour in this figure legend, the reader is referred to the web version of this article.)

5. Conclusions

In this paper, we have presented a 2D cellular automaton (CA) model with the dynamic Monte Carlo (DMC) method to investigate the crowd evacuation dynamics. This study is driven by the rising need on understanding the mechanisms of how pedestrians exit a building. So we can develop a quantitative method to help to design pedestrian facilities and control pedestrian flow in case of emergency to reduce the injuries and casualties during evacuation. The proposed CA model incorporates stochastic rules to describe pedestrians' movements and their interactions.

We implemented an efficient DMC method with fast searching for selecting transition events to simulate the evacuation process. In the DMC algorithm, the movements and interactions of individuals are characterized by the transition rates depending on the distance from each individual to the exit and the distances from their neighboring sites to the exit. Then, the corresponding time it takes to evolve the dynamics can be determined by using these rates. Therefore, we can apply the DMC method to predict the evacuation time quantitatively. We also note that the Metropolis Monte Carlo (MMC) algorithm could be used to reproduce an equilibrium state of a system, but the DMC algorithm is more appropriate to simulate the evacuation dynamics. Furthermore, because the DMC method is "rejection-free", it can be taken as one contribution with regard to the computational efficiency.

With the DMC method, we established and validated our CA model, which can illustrate the characteristics of pedestrian dynamics during the evacuation and estimate the evacuation time for different room sizes, exit widths, and initial densities. In our results, we find that the evacuation time increases almost linearly with the initial density of pedestrians. When the exit width gets bigger, the evacuation time decreases. The simulations also show some observed patterns of the evacuating crowds, for example, the pedestrian arch formation and clogging around an exit.

In this paper, we propose the model in a square or rectangular room with one or two exits, and all the pedestrians behave in the same way with the same walking speed. We have not included more complex components into the model, for instance, obstacles in the room, different individual behaviors (e.g., unequal moving speeds), limited visibility of the room, and the herding effect [56,57]. In the future, we plan to explore how to modify our model and adapt the DMC algorithm for these aspects.

Data availability

Data will be made available on request.

Acknowledgments

We would like to thank the two anonymous referees for their valuable comments and suggestions for improvement. We acknowledge support from the NSF grants DMS-1913146, DMS-1954532 and DMS-2208467, a South Carolina EPSCoR GEAR-CRP award (20-GC04), and the USC ASPIRE grants (2019-2021, 2022-2023).

References

- [1] J. Gill, K. Landi, Traumatic asphyxial deaths due to an uncontrolled crowd, Am. J. Forensic Med. Pathol. 25 (2004) 358-361.
- [2] R.S. Lee, R.L. Hughes, Prediction of human crowd pressures, Accid. Anal. Prev. 38 (2006) 712–722.
- [3] C. Ahn, J. Kim, S. Lee, An analysis of evacuation under fire situation in complex shopping center using evacuation simulation modeling, Procedia-Soc. Behav. Sci. 218 (2016) 2434.
- [4] D. Helbing, I. Farkas, T. Vicsek, Simulating dynamical features of escape panic, Nature 407 (2000) 487-490.

- [5] A. Schadschneider, Traffic flow: a statistical physics point of view, Physica A 313 (2002) 153-187.
- [6] C. Castellano, S. Fortunato, V. Loreto, Statistical physics of social dynamics, Rev. Mod. Phys. 81 (2009) 591-646.
- [7] N. Bellomo, C. Dogbe, On the modeling of traffic and crowds: a survey of models, speculations, and perspectives, SIAM Rev. 53 (2011) 409-463.
- [8] A. Schadschneider, D. Chowdhury, K. Nishinari, Stochastic Transport in Complex Systems, Elsevier, The Netherlands, 2011.
- [9] D.C. Duives, W. Daamen, S.P. Hoogendoorn, State-of-the-art crowd motion simulation models, Transp. Res. C 37 (2013) 193–209.
- [10] H. Vermuyten, J. Beliën, L.D. Boeck, G. Reniers, T. Wauters, A review of optimisation models for pedestrian evacuation and design problems, Saf. Sci. 87 (2016) 167–178.
- [11] D. Helbing, A fluid dynamic model for the movement of pedestrians, Complex Syst. 6 (1992) 391-415.
- [12] R.L. Hughes, A continuum theory for the flow of pedestrians, Transp. Res. B 36 (2002) 507-535.
- [13] A. Chertock, A. Kurganov, A. Polizzi, I. Timofeyev, Pedestrian flow models with slowdown interaction, Math. Models Methods Appl. Sci. 24 (2014) 249-275.
- [14] U. Weidmann, U. Kirsch, M. Schreckenberg, Pedestrian and Evacuation Dynamics, Springer, Berlin, 2014.
- [15] F.E. Cornes, G.A. Frank, C.O. Dorso, High pressures in room evacuation processes and a first approach to the dynamics around unconscious pedestrians, Physica A 484 (2017) 282-298.
- [16] Y.B. Han, H. Liu. Modified social force model based on information transmission toward crowd evacuation simulation. Physica A 469 (2017) 499–509.
- [17] H. Zhang, H. Liu, X. Qin, B.X. Liu, Modified two-layer social force model for emergency earthquake evacuation, Physica A 492 (2018) 1107–1119.
- [18] G. Köster, F. Treml, M. Gödel, Avoiding numerical pitfalls in social force models, Phys. Rev. E 87 (2013) 063305.
- [19] S. Wolfram, Theory and Applications of Cellular Automata, World Scientific, Singapore, 1986.
- [20] S. Wolfram, Cellular Automata and Complexity, Addison-Wesley, Reading, MA, 1994.
- [21] S. Wolfram, A New Kind of Science, Wolfram Media, Champaign, IL, 2002.
- [22] C. Burstedde, K. Klauck, A. Schadschneider, J. Zittarz, Simulation of pedestrian dynamics using a two-dimensional cellular automaton, Physica A 295 (2001) 507-525.
- [23] A. Kirchner, A. Schadschneider, Simulation of evacuation processes using a bionics-inspired cellular automaton model for pedestrian dynamics, Physica A 312 (2002) 260-276.
- [24] C. Saloma, G.J. Perez, G. Tapang, M. Lim, C. Palmes-Saloma, Self-organized queuing and scale-free behavior in real escape panic, Proc. Natl. Acad. Sci. USA 100 (2003) 11947-11952.
- [25] M. Isobe, D. Helbing, T. Nagatani, Experiment, theory, and simulation of the evacuation of a room without visibility, Phys. Rev. E 69 (2004) 066132.
- [26] S. Bouzat, M.N. Kuperman, Game theory in models of pedestrian room evacuation, Phys. Rev. E 89 (2014) 032806.
- [27] L. Wang, Y. Jiang, Escape dynamics based on bounded rationality, Physica A 531 (2019) 121777.
- [28] Z.-H. Chen, Z.X. Wu, J.Y. Guan, Twofold effect of self-interest in pedestrian room evacuation, Phys. Rev. E 103 (2021) 062305.
- [29] Y. Li, M. Chen, Z. Dou, X. Zheng, Y. Cheng, A. Mebarki, A review of cellular automata models for crowd evacuation, Physica A 526 (2019) 120752.
- [30] W. Song, X. Xu, B.-H. Wang, S. Ni, Simulation of evacuation processes using a multi-grid model for pedestrian dynamics, Physica A 363 (2006) 492-500.
- [31] S. Cao, W. Song, W. Lv, Z. Fang, A multi-grid model for pedestrian evacuation in a room without visibility, Physica A 436 (2015) 45-61.
- [32] H. Ren, Y. Yan, F. Gao, Variable guiding strategies in multi-exits evacuation: pursuing balanced pedestrian densities, Appl. Math. Comput. 397 (2021)
- [33] L. Lu, C. Chan, J. Wang, W. Wang, A study of pedestrian group behaviors in crowd evacuation based on an extended floor field cellular automaton model, Transp. Res. Part C Emerg. Technol. 81 (2017) 317-329.
- X. Li, F. Guo, H. Kuang, Z. Geng, Y. Fan, An extended cost potential field cellular automaton model for pedestrian evacuation considering the restriction of visual field, Physica A 515 (2019) 47-56.
- [35] C. Henein, T. White, Macroscopic effects of microscopic forces between agents in crowd models, Physica A 373 (2007) 694-712.
- [36] J. Wang, L. Zhang, Q. Shi, P. Yang, X. Hu, Modeling and simulating for congestion pedestrian evacuation with panic, Physica A 428 (2015) 396-409.
- [37] L. Zheng, X. Peng, L. Wang, D. Sun, Simulation of pedestrian evacuation considering emergency spread and pedestrian panic, Physica A 522 (2019) 167-181.
- [38] J. Yi, S. Pan, Q. Chen, Simulation of pedestrian evacuation in stampedes based on cellular automaton model, Simulat. Model. Pract. Theor. 104 (2020)
- [39] J. Kim, C. Ahn, S. Lee, Modeling handicapped pedestrians considering physical characteristics using cellular automaton, Physica A 510 (2018) 507-517.
- [40] Y. Zheng, X. Li, N. Zhu, B. Jia, R. Jiang, Evacuation dynamics with smoking diffusion in three dimension based on an extended floor-field model, Physica A 507 (2018) 414-426.
- [41] J. Tanimoto, A. Hagishima, Y. Tanaka, Study of bottleneck effect at an emergency evacuation exit using cellular automata model, mean field approximation analysis, and game theory, Physica A 389 (2010) 5611-5618.
- [42] A.B. Bortz, M.H. Kalos, J.L. Lebowitz, A new algorithm for Monte Carlo simulation of ising spin systems, J. Comput. Phys. 17 (1975) 10-18.
- [43] K.A. Fichthorn, W.H. Weinberg, Theoretical foundations of dynamical Monte Carlo simulations, J. Chem. Phys. 95 (1991) 1090–1096.
 [44] N. Metropolis, A.E. Rosenbluth, M.N. Rosenbluth, A.H. Teller, E. Teller, Equation of state calculations by fast computing machines, J. Chem. Phys. 21 (1953) 1087-1091.
- [45] Y. Sun, I. Timofeyev, Kinetic Monte Carlo simulations of 1D and 2D traffic flows: comparison of two look-ahead rules, Phys. Rev. E 89 (2014) 052810.
- [46] Y. Sun, Kinetic Monte Carlo simulations of two-dimensional pedestrian flow models, Physica A 505 (2018) 836–847.
- [47] Y. Sun, Simulations of bi-direction pedestrian flow using kinetic Monte Carlo methods, Physica A 524 (2019) 519-531.
- [48] Y. Sun, Kinetic Monte Carlo simulations of bi-direction pedestrian flow with different walk speeds, Physica A 549 (2020) 124295.
- [49] Y. Sun, C. Tan, On a class of new nonlocal traffic flow models with look-ahead rules, Physica D 413 (2020) 132663.
- [50] T.D. Liggett, Interacting Particle Systems, Springer, Berlin, 2005. Reprint
- [51] A. Sopasakis, M.A. Katsoulakis, Stochastic modeling and simulation of traffic flow: asymmetric single exclusion process with arrhenius look-ahead dynamics, SIAM J. Appl. Math. 66 (2006) 921-944.
- C. Chen, H. Sun, P. Lei, D. Zhao, C. Shi, An extended model for crowd evacuation considering pedestrian panic in artificial attack, Physica A 571 (2021)
- [53] S. Buchmueller, U. Weidmann, Parameters of pedestrians, pedestrian traffic and walking facilities, Schriftenreihe des IVT 132, ETH Zürich, 2007,
- [54] J. Guan, K. Wang, Cooperative evolution in pedestrian room evacuation considering different individual behaviors, Appl. Math. Comput. 369 (2020) 124865
- F.Y. Guo, H.J. Huang, A mobile lattice gas model for simulating pedestrian evacuation, Physica A 387 (2008) 580-586.
- [56] G. Albi, M. Bongini, E. Cristiani, D. Kalise, Invisible control of self-organizing agents leaving unknown environments, SIAM J. Appl. Math. 76 (2016)
- [57] A. Ciallella, E.N.M. Cirillo, P.L. Curseu, A. Muntean, Free to move or trapped in your group: mathematical modeling of information overload and coordination in crowded populations, Math. Models Methods Appl. Sci. 28 (2018) 1831-1856.